

Dynamics of Soil Water and Temperature in Aboveground Sand Cultures Used for Screening Plant Salt Tolerance

D. Wang*

ABSTRACT

There are increasing concerns about the feasibility of applying plant salt tolerance information obtained from artificial sand cultures in field soils. A main question concerns the similarity of growth conditions between the sand cultures and the field. This study was conducted to determine the dynamic variations of soil water and temperature in sand cultures and to compare them with the same parameters observed in a field soil. Results indicated that sand cultures filled with a reasonably well graded river sand exhibited values of minimum and maximum soil water content similar to those in the field. Soil volumetric heat capacity and thermal conductivity of the river sand were also comparable with values found in the field soil. A poorly graded silica sand, however, was found not suitable to reproduce soil water and temperature regimes that commonly occur in the field. If other environmental factors for plant growth can be simulated to match those found in the field, results of plant salt tolerance obtained from the sand cultures can be used to provide guidance for plant selection under field conditions. The approach of using particle-size analysis information to derive the hydraulic and thermal properties should be readily adoptable by interested researchers in selecting the most appropriate grading of sand culture materials.

ROOT-ZONE SALINITY is one of the major production and environmental concerns in irrigated agriculture, especially in arid regions. High levels of salinity caused by elevated salt concentrations in soil solution can severely impair plant growth resulting in significant yield losses. A survey of salinity effects on agricultural and horticultural crops indicates that salt sensitive species have threshold tolerance values as low as 1.5 dS m^{-1} , whereas tolerant species may reach 10 dS m^{-1} in the saturation extract (Maas and Hoffman, 1977). The high salt content in soil and water also poses a potential threat to surface and ground water quality.

The concept of root-zone salinity or profile-averaged salinity (Wu et al., 2001) and its application to plant studies often assumes a pseudostatic condition where growth and yield responses are referenced to a salinity value averaged over the entire root zone. However, the soluble salt concentration in the soil is a dynamic function of soil texture, structure, porosity, bulk density, soil water content, and soil temperature. The discrepancy between a single value of average root-zone salinity and its variable nature in field soils has long been recognized (Shannon, 1979). Further, spatial and temporal variability in soil salinity creates additional difficulties in plant salt tolerance assessment studies in field soils. A possible alternative to these difficulties is to use artificial sand cultures irrigated with nutrient solutions that are salinized to prescribed salinity levels (Grieve and Shannon, 1999). Frequent irrigation and careful selection of the sand materials can provide root-zone salinity values relatively constant over time and soil depths.

Although the application of a fixed-level salinity as the primary treatment variable, often by means of irrigation with saline water (Shani and Dudley, 2001), has many practical agronomic advantages for studying plant salt tolerance, whole plant response to salt stress is convoluted by environmental variables such as temperature, humidity, radiation, and soil water content that coaffect both transpiration and growth (Baker et al., 1992). Dalton and Poss (1989) showed that the threshold values of root-zone salinity are related to soil temperature. For most plant species, there exists an optimal soil temperature for root growth (McMichael and Burke, 1996). The interactive and overlapping effect of soil temperature on plant growth should be integrated in plant salt tolerance assessment studies. A dynamic salinity stress index was proposed by Dalton et al. (1997) to account for temperature and other biophysical variables, in addition to salinity, that are important to root water uptake.

Despite the obvious advantages of using sand cultures for screening plant salt tolerance, the artificial growth environment is often far from duplicating the biophysical growth conditions in the field. Two of the most important variables are soil water content and soil temperature. The objectives of the reported study were: (i) to determine the dynamics of soil water and soil temperature in aboveground sand cultures, and (ii) to compare with the soil water and thermal regimes of a field soil in the context of selection criteria of appropriate sand materials and feasibility assessment of transferring plant salt tolerance information from sand cultures to the field.

MATERIALS AND METHODS

The Sand Culture Experiments

The sand cultures used in this study were black high-strength polyvinyl containers, 120 by 60 by 45 cm for the length, width, and height dimensions, that were filled with a number 12 silica sand for Exp. 1 and a washed river sand for Exp. 2. The silica sand was a high-purity quartz (SiO_2) that has often been used as a uniform porous medium to support plant growth or for chemical transport studies (Meeussen et al., 1999), whereas the washed river sand that provides some particle-size separation has primarily been used as a growth medium for plant assessment studies (Grieve and Shannon, 1999). Irrigation of these sand cultures or sand tanks was accomplished through small closely spaced openings on polyvinyl chloride (PVC) pipes fitted on the inside edge along the 120-cm sides (Fig. 1). These sand tanks were preexisting and operational facilities

Dep. of Soil, Water, and Climate, Univ. of Minnesota, St. Paul, MN 55108. Received 18 Oct. 2001. *Corresponding author (dwang@soils.umn.edu).

Published in Soil Sci. Soc. Am. J. 66:1484–1491 (2002).

Abbreviations: C_s , soil volumetric heat capacity; TDR, time domain reflectometry.

that were located in greenhouses equipped with automated climate control systems. Nonsaline irrigation water ($<1 \text{ dS m}^{-1}$) was pumped, within a closed system, to the surface of the sand tanks from 687-L reservoirs located at a lower level of the greenhouses, percolated through the sands, then drained back to the reservoirs by gravity. For Exp. 1 with the silica sand, the recirculating irrigation was carried out three times a day at 0830, 1130, and 1430 h, with each irrigation lasting for 12 min. For Exp. 2 with the river sand, four irrigation runs were used at 0830, 1130, 1430, and 1730 h, with each irrigation lasting for 10 min. The increased frequency and reduced duration in the river sand was intended to account for the texture differences that resulted in a reduced water intake rate compared with the silica sand.

Soil water content and soil temperature were measured using time domain reflectometers (CS615) and thermocouple probes (105T) from Campbell Scientific Inc. Two banks of CS615 sensors were installed, with one bank near the edge and the other near the center of the sand tank, at 2-, 5-, 10-, 20-, 30-, and 40-cm depths, respectively (Fig. 1). The temperature probes were installed on the other half of the same cross-section and additional probes were placed at the sand surface. Because of the potentially very rapid infiltration rate, a 5-s sampling interval was used in the dataloggers to record both soil water content and soil temperature. Replicated sand samples were taken before and after each experiment for the determination of bulk density and particle-size distribution for the two sand media.

The Field Experiment

A separate field experiment was conducted that focused primarily on salinity, irrigation management, soil water content, and soil temperature among other key biophysical parameters for optimized soybean growth. Results from drip-irrigation treatments of the field experiment were used, where the drip irrigation system, similar to that described in Aragüés et al. (1999), was set up to facilitate salt injection to selective levels of salinity. To compare with the sand culture experiments, however, only measurements from the nonsaline treatment were used. The irrigation water was low in salinity ($<1 \text{ dS m}^{-1}$). The soil at the field site was an Arlington fine sandy loam (coarse-loamy, mixed, thermic, Haplic Durixeralf) that consisted of about 64% sand, 99.1% total mineral materials, and 0.9% organic matter.

To measure soil water content and soil temperature, time domain reflectometry (TDR) probes and the 105T thermocouples were installed at separate sections beneath field rows. The installation was accomplished by excavating trenches traversing the field row and inserting the probes into the undisturbed soil at predetermined depths (5, 10, 20, 30, and 50 cm). The trenches were backfilled with the same soil to restore conditions similar to that before the excavation and left for several irrigation cycles for hydraulic equilibrium before starting to collect data. The TDR probes were read with a 1502 B Tektronix cable tester (Tektronix, Beaverton, OR) with the Campbell SDM1502 communication interface and a SDMX50 multiplexer controlled through a CR10X datalogger from Campbell Scientific. The TDR setup was calibrated in the laboratory against gravimetric water content measurements using the same field soil under five volumetric moisture contents. Replicated soil samples were also taken for bulk density determination and particle-size distribution analysis.

Analyses of Particle and Pore Sizes, Capillary Potential, and Thermal Properties

Based on the particle-size analysis data, a fraction-weighted equivalent mean particle radius (R_p) was determined as

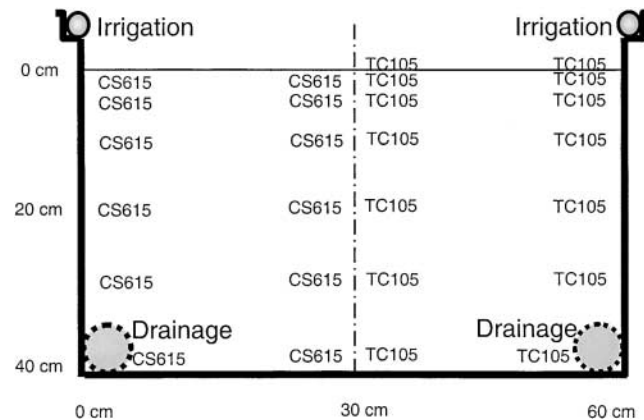


Fig. 1. Schematic of a cross-section of the sand tanks and installation of soil water content and soil temperature sensors.

$$R_p = \sum_{i=1}^m [r_i f_{r_i}] \quad [1]$$

where r_i was the average particle radius (mm) for a size range i (equal to the average value between two adjacent sieve sizes, i.e., $i - 1$ and i or i and $i + 1$), m equals the total number of size classes minus 1, f_{r_i} equals the weight fraction of class range i over the total weight of the m classes and $\Sigma(f_{r_i}) = 1$.

An equivalent mean pore or void radius (R_v) was estimated using the semi-empirical model of Arya and Paris (1981)

$$R_v = R_p \sqrt{\frac{2}{3}} e^{n^{(1-\alpha)}} \quad [2]$$

where e was the void ratio and defined as $(\rho_p - \rho_b)/\rho_b$, $n = (\rho_b/\rho_p)/(4\pi R_p^3/3)$, ρ_p and ρ_b were respectively the particle and bulk density, and the empirical parameter α was maintained as a constant value of 1.38 (Arya and Paris, 1981) for all three texture classes.

The matric or capillary potential (P_c) corresponding to the mean equivalent pore sizes was computed as

$$P_c = -\frac{2\sigma \cos(\beta)}{R_v} \quad [3]$$

where σ was the soil water surface tension ($= 73 \text{ g s}^{-2}$), β was the water contact angle (degrees) and was assumed to be zero.

Soil volumetric heat capacity (C_s) was calculated as

$$C_s = f_q \rho_q c_q + f_m \rho_m c_m + f_o \rho_o c_o + \theta \rho_w c_w \quad [4]$$

where f represented volume fraction, ρ = density (g cm^{-3}), c equals the specific heat ($\text{J g}^{-1} \text{C}^{-1}$), θ was the volumetric soil water content ($\text{cm}^3 \text{cm}^{-3}$), and subscripts q, m, o, w represented quartz, soil minerals, organic matter, and water content, respectively. Values of specific heat were 0.80, 0.87, 1.92, and $4.18 \text{ J g}^{-1} \text{C}^{-1}$ for quartz, soil minerals, organic matter, and water, respectively (Campbell and Norman, 1998). Contributions of soil air to C_s were negligible and ignored in the calculations.

Soil thermal conductivity (k_s) was calculated based on a fraction- and efficiency-weighted contribution from different soil constituents (De Vries, 1963)

$$k_s = \frac{f_q \xi_q k_q + f_m \xi_m k_m + f_o \xi_o k_o + \theta \xi_w k_w + f_g \xi_g k_g}{f_q \xi_q + f_m \xi_m + f_o \xi_o + \theta \xi_w + f_g \xi_g} \quad [5]$$

where ξ represented weighting factors for various soil constituents, subscript g was for soil gas (air and water vapor), and k with different subscripts represented thermal conductivity values of each soil constituent. Values of k were 8.8, 2.5, 0.25, 0.6, and $0.074 \text{ W m}^{-1} \text{C}^{-1}$ for quartz, soil minerals, organic mat-

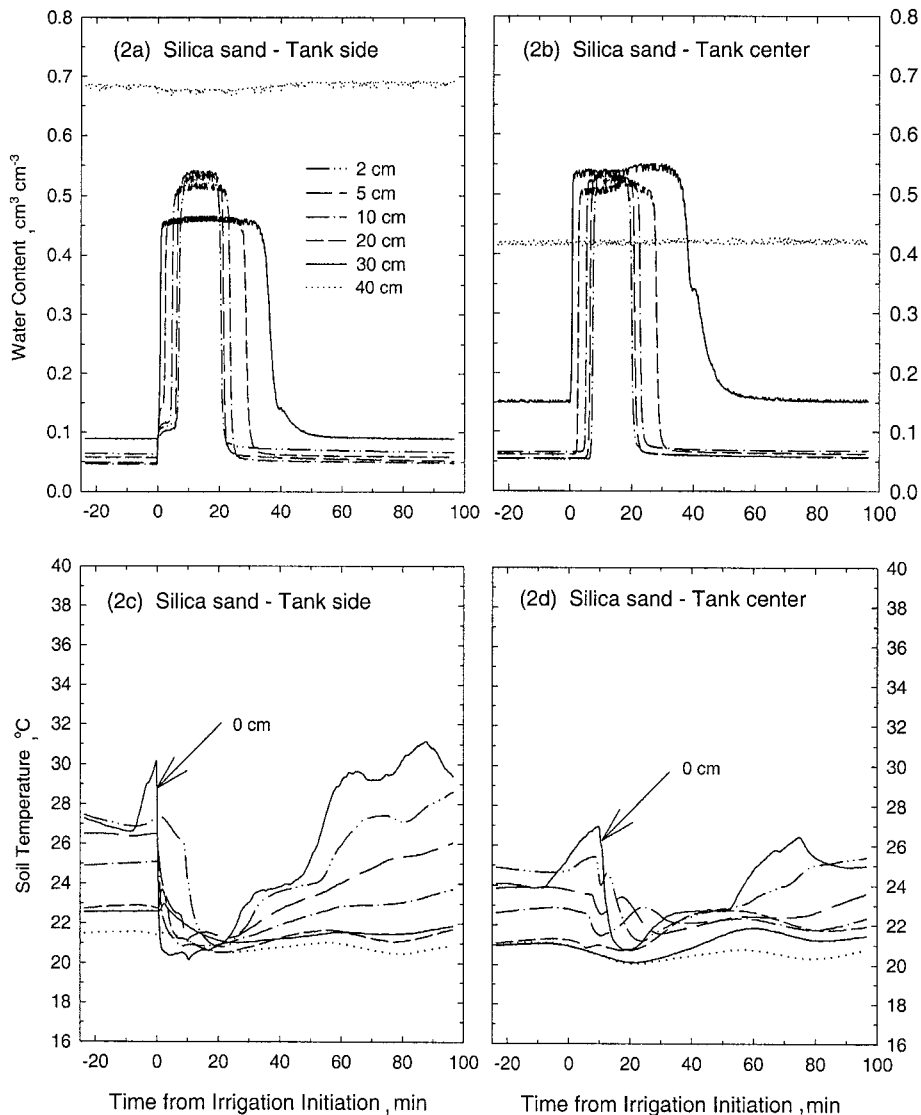


Fig. 2. Soil water content (a, b) and temperature (c, d) during an irrigation event in a tank filled with a silica sand.

ter, water, and moist soil air, respectively (Campbell and Norman, 1998). The weighting factors (ξ) were estimated using a fluid conductivity (Campbell et al., 1994) and a set of functions from Campbell and Norman (1998).

Clearly, values of both the heat capacity and thermal conductivity are dynamic functions of soil water content. Because soil mineral and organic components should remain relatively constant, to represent the extreme cases, values of the heat capacity and thermal conductivity were computed for soil water content averaged for the top 20-cm depth before an irrigation event when water content was the smallest (θ_{\min}) and near the end of an irrigation when the water content reached the highest values (θ_{\max}).

RESULTS AND DISCUSSION

Soil Water and Temperature Regimes

In the silica sand, the surface irrigation water percolated instantly to the bottom of the tanks, without lateral movement at the sand surface (Fig. 2a). The surface drip or flood irrigation became virtually subsurface irrigation where an incremental increase in water content (from

bottom up) followed the rising water table recharged by the irrigation water. The minimum soil water content prior to irrigation was about $0.06 \text{ cm}^3 \text{ cm}^{-3}$ and the maximum water content reached $0.52 \text{ cm}^3 \text{ cm}^{-3}$ during irrigation. The lower readings at the 20- and 30-cm depths and the persistently higher values at the 40-cm depth were attributed to boundary effects where the sensors were measuring, in addition to soil water, the drainage pipes and the water inside the drain that acted as a water table (Fig. 1). After irrigation, soil water content decreased rapidly to values close to those prior to the irrigation event, and the reduction followed a reverse order (from top down) caused by the receding water table. Similar wetting and drainage patterns were observed at the tank center (Fig. 2b). However, the maximum soil water content at the 20- and 30-cm depths reached similar values as those at shallower depths because of the absence of the drainage pipes. The water content at the 40-cm depth remained at about $0.42 \text{ cm}^3 \text{ cm}^{-3}$, unchanged during the course of the irrigation, which indicated a residual water

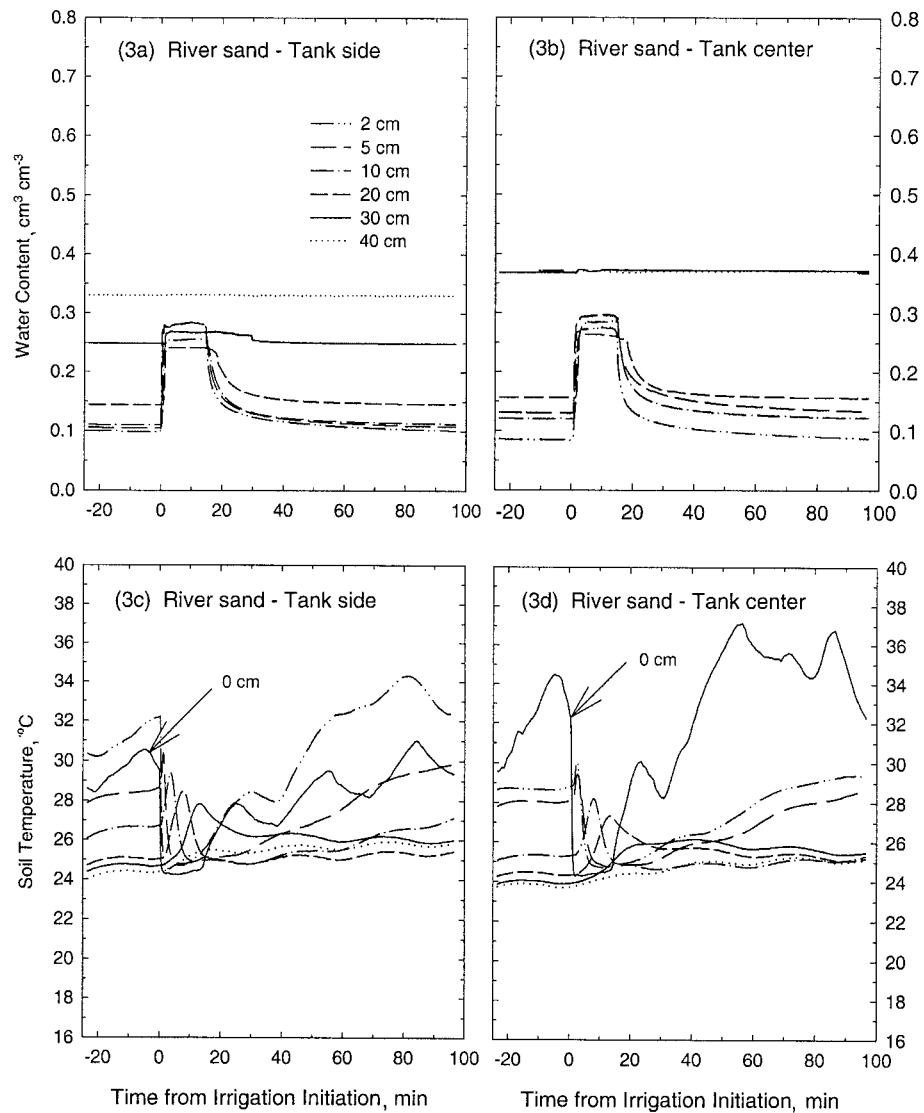


Fig. 3. Soil water content (a, b) and temperature (c, d) during an irrigation event in a tank filled with a washed river sand.

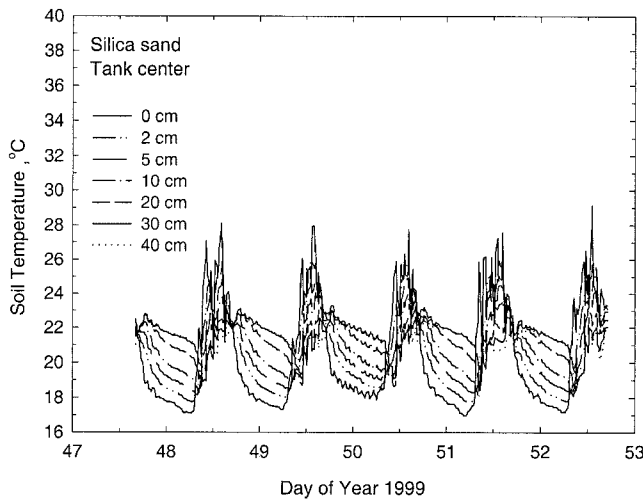


Fig. 4. Soil temperature at different depths during a 5-d period in a tank filled with silica sand.

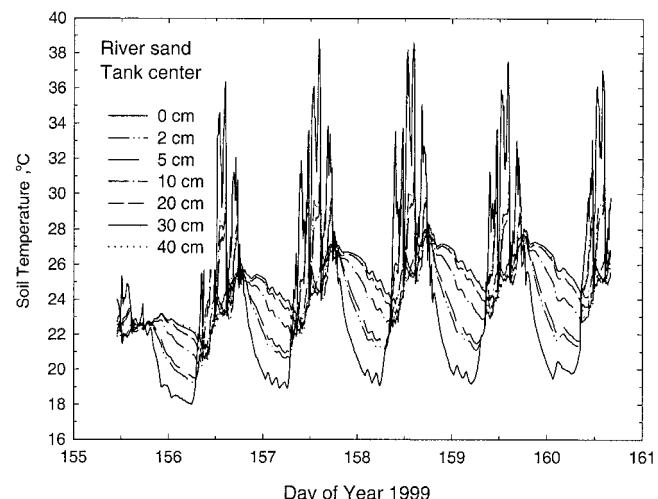


Fig. 5. Soil temperature at different depths during a 5-d period in a tank filled with washed river sand.

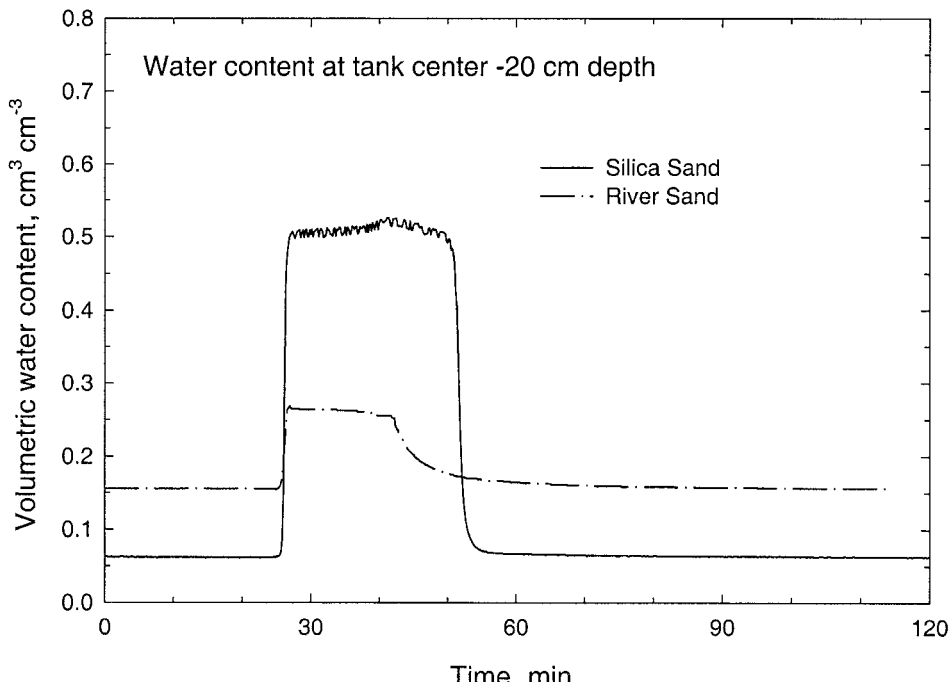


Fig. 6. Comparison of soil water content between silica sand and river sand at the 20-cm depth.

table at a height within the sensing range of the 40-cm soil water probe.

Affected by the irrigation water, soil surface temperature immediately decreased to water temperature ($\sim 20^\circ\text{C}$) at the tank side (Fig. 2c). The reduction of soil temperature of other depths and at the tank center followed the same order as the water content changes (Fig. 2c,d). Comparing values from the same soil depth, soil temperature prior to irrigation was 1 to 3°C higher at the tank side than at the center locations because of heat transfer from the ambient air and through the tank walls. Because of this additional heat source, the rate of temperature recovery was also faster at the tank side than at the center locations.

In the river sand experiment, changes in soil water content in the wetting process (Fig. 3a,b) exhibited patterns similar to the silica sand. However, the desatura-

tion or drainage cycles required considerably longer time than in the silica sand. Some lateral water flow on the surface was also observed and a less pronounced temporal separation in water content increase by depth was recorded by the water content sensors. The minimum soil water content prior to irrigation was about $0.13 \text{ cm}^3 \text{ cm}^{-3}$ and the maximum water content reached only $0.28 \text{ cm}^3 \text{ cm}^{-3}$ during irrigation. The range between the minimum and maximum water content in the river sand was very similar to water content variations commonly observed in field soils. Similar to the silica sand, soil temperature in the river sand was reduced by the irrigation water. However, the order of temperature reduction started from the surface at both the tank side and center locations (Fig. 3c,d). The order of temperature reduction was also consistent with the water content measurement. The absolute values of surface temperature and water temperature were different from the silica sand experiment because the river sand experiment was conducted in a different greenhouse and at a later season of the year when the daily mean temperature was higher (Fig. 4 and 5). The maximum diurnal temperature variation at the surface was between 17 to 28°C in the silica sand (Fig. 4) and 18 to 38°C in the river sand (Fig. 5). Large temperature variations, similar to that in the river sand, are often observed in field soils. Unlike field soils, however, the smaller phase lag in temperature changes over depth, especially in the silica sand, indicated potentially low values in heat capacity and high thermal conductivity. A direct comparison using measurements at the 20-cm depth further demonstrated that soil water content of the two sand materials responded similarly in the wetting process but with different minimum and maximum water content values (Fig. 6). The comparison also depicted that the drainage process took much

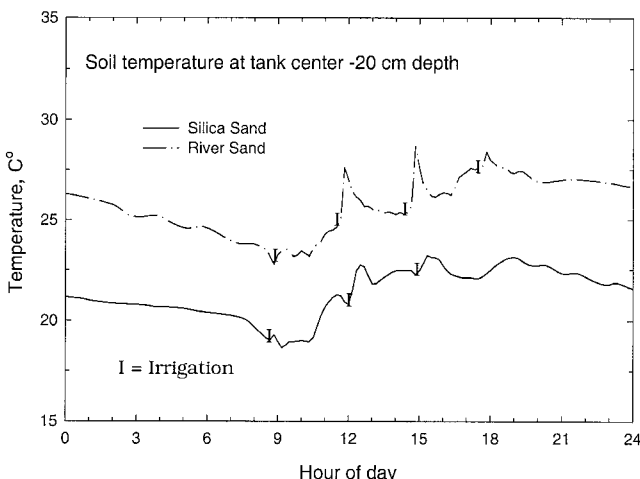


Fig. 7. Comparison of soil temperature between silica sand and river sand at the 20-cm depth.

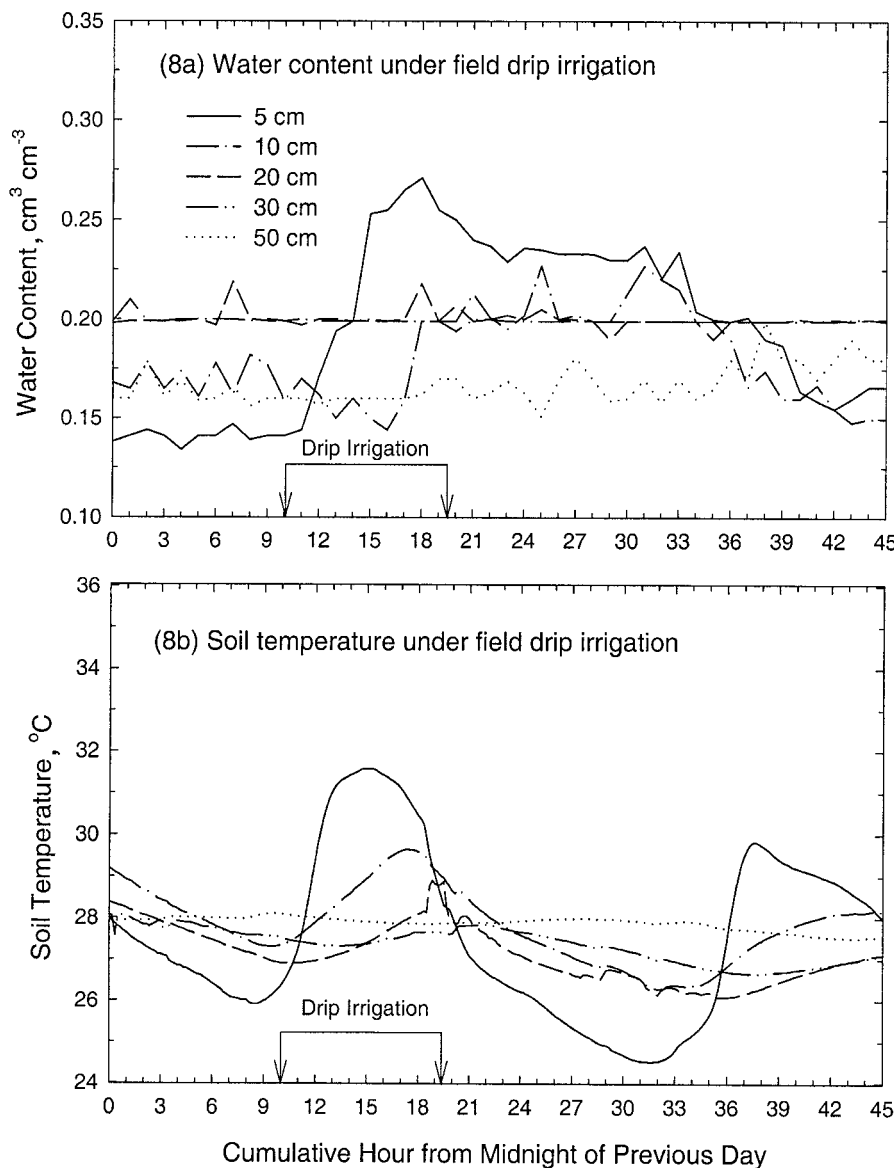


Fig. 8. Soil water content (a) and temperature (b) in a field soil during a drip irrigation event.

longer time in the river sand (about 30 min) than in the silica sand (about 5 min). Furthermore, the daytime surface irrigation generated a small heat pulse from surface layers that translated to a slight temperature increase at the 20-cm depth (Fig. 7).

In the field experiment, soil water content at only the 5- and 10-cm depths responded to each drip irrigation event (Fig. 8a). The increase in water content at the 10 cm depth lagged the increases at the 5-cm depth by ~5 h. The water content at the 5-cm depth increased from a low value of $0.14 \text{ cm}^3 \text{cm}^{-3}$ prior to irrigation to a maximum value of $0.27 \text{ cm}^3 \text{cm}^{-3}$ during the irrigation. The range of variation was very similar to that in the river sand. Temperature in the field soil did not respond to the irrigation (Fig. 8b). Relatively large phase lags in temperature change over depth were also found, compared with the sand cultures. The slower or gradual temperature change over depth was likely attributable to

larger heat capacity values in the field soil than in the sand materials.

Particle-Size Distribution and Parameter Comparison

Particle sizes and distribution were significantly different between the two sand materials and the field soil (Fig. 9). As expected, the silica sand had the least

Table 1. Uniformity index, density, equivalent mean particle radius, pore radius, and capillary potential[†].

Soil type	I_u	ρ_p	ρ_b	R_p	R_v	P_c
		— g cm^{-3} —	— mm —	— mm —	— kPa —	
Silica sand	2.7	2.65	1.23	0.88	1.09	-0.13
River sand	14.1	2.65	1.54	0.51	0.35	-0.42
Field soil	52.5	2.65	1.53	0.12	0.03	-4.25

[†] I_u , particle uniformity index ($= d_{50}/d_{10}$); ρ_p , particle density; ρ_b , bulk density; R_p , equivalent mean particle radius; R_v , equivalent mean void or pore radius; P_c , equivalent mean capillary or matric potential.

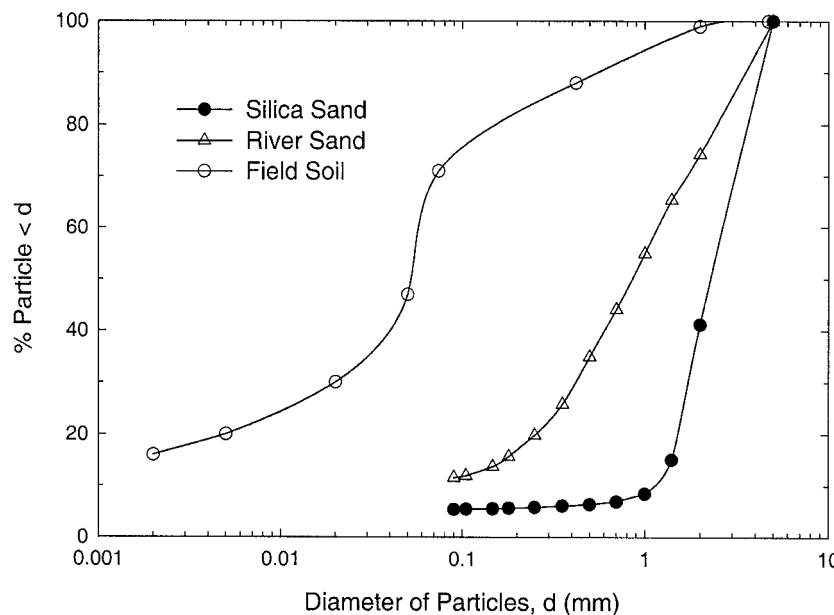


Fig. 9. Particle-size distribution of a silica sand, a river sand, and a field soil.

separation and the field soil exhibited the greatest spread in particle sizes. Consistent with data in Fig. 9, the silica sand had the smallest value for particle uniformity index (I_u), whereas I_u was the largest for the field soil (Table 1). Because the silica sand was nearly 100% quartz, the particle density was assumed to be 2.65 g cm^{-3} . Both the river sand and the field soil consisted of over 99% mineral composition, it was reasonable to assume a particle density of 2.65 g cm^{-3} . Soil bulk density was only 1.23 g cm^{-3} for the silica sand, however, the river sand had a bulk density value nearly identical to that of the field soil (Table 1).

The computed equivalent mean particle radius (R_p) for the silica sand was 0.88 mm or a diameter of 1.76 mm which was remarkably similar to the diameter of 1.7 mm specified by the manufacturer. The estimated equivalent mean void radius (R_v) of the silica sand was about three times that of the river sand, and over 30 times that of the field soil (Table 1). The large differences in void sizes translated to proportional differences in the capillary potential that the soil pores exerted on soil water. After free drainage, higher pore potential such as in the silica sand would hold less amount of water, and lower potential such as in the field soil would hold more water. Soil water content averaged over the top 20-cm depth before an irrigation event was only $0.06 \text{ cm}^3 \text{ cm}^{-3}$ for the silica sand (θ_{\min} in Table 2), but a significantly higher value was found for the field soil ($0.17 \text{ cm}^3 \text{ cm}^{-3}$). Consistent

with the temperature measurements, at $\theta = \theta_{\min}$, estimated C_s of the silica sand was 70% smaller than that of the field soil (Table 2). At θ_{\min} , the C_s value for the river sand was comparable with the field soil. Although C_s increased significantly during water saturation (θ_{\max}) to a value greater than that of the field soil, the short duration of each irrigation event would less likely have a significant effect on the overall soil thermal regime. In the silica sand experiment, the total duration of irrigation or water saturation was 36 min for each 24-h period. Soil thermal conductivity was nearly identical between the river sand and the field soil because of similar mineral composition and similar values of minimum and maximum soil water content. The slightly higher k_s values in silica sand were attributed to (i) the higher particle thermal conductivity for quartz at $\theta = \theta_{\min}$, and (ii) significantly higher water content at $\theta = \theta_{\max}$, compared with the river sand or field soil.

CONCLUSIONS

Analyses of soil water and thermal regimes in sand cultures and comparison with a field soil provided strong evidence to support the application of artificial sand cultures for plant screening studies. A carefully selected sand medium such as the washed river sand would fulfill the need of providing rapid solution exchange to achieve a desired growth condition in the root zone, while main-

Table 2. Soil heat capacity and thermal conductivity†.

Soil type	Volume fraction			Water content		C_s		k_s	
	f_q	f_m	f_o	θ_{\min}	θ_{\max}	θ_{\min}	θ_{\max}	θ_{\min}	θ_{\max}
Silica sand	0.46	0.00	0.00	0.06	0.52	1.23	3.16	1.01	1.57
River sand	0.00	0.58	0.00	0.13	0.28	1.88	2.51	0.94	1.05
Field soil	0.00	0.57	0.01	0.17	0.22	2.04	2.25	0.93	0.99

† f_q , f_m , and f_o are volume fractions of quartz, soil minerals, and organic matter content, respectively; θ_{\min} and θ_{\max} are the average minimum and maximum volumetric water content of the top 20-cm soil, C_s = soil heat capacity, k_s = soil thermal conductivity.

taining hydraulic and thermal properties comparable with field soils. The approach of using simple particle-size analysis data to derive the capillary potential and thermal properties should be readily adoptable by interested researchers in selecting the most appropriate grading of sand culture materials. In actual saline conditions, the analyses may be improved by considering the potential impact of solution salt content on soil thermal conductivity (Noborio and McInnes, 1993). An inherent disadvantage with the sand cultures is the disappearance of soil structure that can have a significant effect on soil hydraulic properties (Nimmo, 1997).

ACKNOWLEDGMENTS

The author thanks Dr. M. Shannon for creating an opportunity to carry out the study and helpful discussions on the experiments. The author was also very grateful to Dr. C. Grieve, T. Donovan, J. Poss, and J. Draper for providing essential assistance in the experiments, and to Dr. J. Baker for helpful comments on the manuscript.

REFERENCES

- Aragüés, R., E. Playán, R. Ortiz, and A. Royo. 1999. A new drip-injection irrigation system for crop salt tolerance evaluation. *Soil Sci. Soc. Am. J.* 63:1397–1403.
- Arya, L.M., and J.F. Paris. 1981. A physicoempirical mode to predict the soil moisture characteristic from particle-size distribution and bulk density data. *Soil Sci. Soc. Am. J.* 45:1023–1030.
- Baker, J.M., J.M. Wraith, and F.N. Dalton. 1992. Root function in water transport. *Adv. Soil Sci.* 19:53–72.
- Campbell, G.S., J.D. Jungbauer, Jr., W.R. Bidlake, and R.D. Hunkerford. 1994. Predicting the effect of temperature on soil thermal conductivity. *Soil Sci.* 158:307–313.
- Campbell, G.S., and J.M. Norman. 1998. An introduction to environmental biophysics. 2nd ed., Springer-Verlag, New York.
- Dalton, F.N., and J.A. Poss. 1989. Water transport and salt loading: a unified concept of plant response to salinity. *Acta Hortic.* 278: 187–193.
- Dalton, F.N., A. Maggio, and G. Piccinni. 1997. Effect of root temperature on plant response functions for tomato: comparison of static and dynamic salinity stress indices. *Plant Soil* 192:307–319.
- De Vries, D.A. 1963. Thermal properties of soils. p. 210–235. *In* W.R. van Wijk (ed.) *Physics of plant environment*. North-Holland Publ. Co., Amsterdam, the Netherlands.
- Grieve, C.M., and M.C. Shannon. 1999. Ion accumulation and distribution in shoot components of salt-stressed Eucalyptus clones. *J. Am. Soc. Hort. Sci.* 124:559–563.
- Maas, E.V., and G.J. Hoffman. 1977. Crop salt tolerance—Current assessment. *J. Irrig. Drain. Div., Am. Soc. Civ. Eng.* 103:115–134.
- McMichael, B.L., and J.J. Burke. 1996. Temperature effect on root growth. p. 383–396. *In* Y. Waisel et al. (ed.) *Plant roots: The hidden half*. 2nd ed. Marcel Dekker, New York.
- Meeussen, J.C.L., J. Kleikemper, A.M. Scheidegger, M. Borkovec, E. Paterson, W.H. van Riemsdijk, and D.L. Sparks. 1999. Multicomponent transport of sulfate in a goethite-silica sand system at variable pH and ionic strength. *Environ. Sci. Technol.* 33:3443–3450.
- Nimmo, J.R. 1997. Modeling structural influences on soil water retention. *Soil Sci. Soc. Am. J.* 61:712–719.
- Noborio, K., and K.J. McInnes. 1993. Thermal conductivity of salt-affected soils. *Soil Sci. Soc. Am. J.* 57:329–334.
- Shani, U., and L.M. Dudley. 2001. Field studies of crop response to water and salt stress. *Soil Sci. Soc. Am. J.* 65:1522–1528.
- Shannon, M.C. 1979. In quest of rapid screening techniques for plant salt tolerance. *HortScience* 14:587–589.
- Wu, L., T.H. Skaggs, P.J. Shouse, and J.E. Ayars. 2001. State space analysis of soil water and salinity regimes in a loam soil underlain by shallow groundwater. *Soil Sci. Soc. Am. J.* 65:1065–1074.